A Compact Multiband BPF Using Step-impedance Resonators with Interdigital Capacitors

Suwaluck MEESOMKLIN [1], Pongsathorn CHOMTONG [2], Prayoot AKKARAEKTHALIN [1]

[1] Dept. of Electrical and Computer Engineering, Faculty of Engineering,
[2] Dept. of Teacher Training in Electrical Engineering, Faculty of Technical Education,
King Mongkut's University of Technology North Bangkok, 1518 Pracharat 1 Road, Bangsue, Bangkok, Thailand

pinkkmutnb@hotmail.com, pongsathornc@kmutnb.ac.th, prayoot@kmutnb.ac.th

Manuscript received January 13, 2016

Abstract. *A compact multiband band-pass filter design for applications of GSM, Wi-MAX and WLAN systems is presented. The design is based on the resonant characteristics of step-impedance and interdigital capacitor resonators with overlap cross coupling structure. The fabricated filter has been operated at the fundamental, first and second harmonic resonant frequencies of 1.8 GHz, 3.7 GHz, and 5.2 GHz, respectively. The experimental results of the fabricated filter agree very well with the simulation expectations using IE3D package. The proposed filter has good performances, while the resonator size can be reduced from λ/2 to λ/8, resulting in the most compact multiband band-pass filter compared with the others using transmission line resonators .*

Keywords

Multiband BPF, step-impedance resonator, interdigital capacitor, overlap cross coupling

1. Introduction

Nowadays, wireless communications are necessary in daily life. Filter is the device that can remove or reject needless signals. It is an important component in RF front-end for both transmitter and receiver. There are four types of filters including high-pass filter, low-pass filter, band-pass filter and band-stop filter. Band-pass filter (BPF) is one popular filter because it can operate from lower cutoff frequency to higher cutoff frequency. The band-pass filters can be developed from different materials and structures. Microstrip is a proper design because of its characteristics; simple design, lighter weight, lower cost, compact size and higher operating frequency range. Most of wireless systems can be operated in two or more frequency bands. More advanced techniques were applied to design band-pass filters such as step-impedance resonators (SIR) used to control harmonic frequencies as desired in dual band BPFs with hairpin structure [1], comb structure [2], and parallel-couple structure [3]. The triple-band BPFs were developed using tri-section step-impedance resonator (TSSIR) with inter-coupled hairpin structure to reduce size and obtain high out of band suppression [4], open stub-embedded TSSIRs arranged in anti-parallel coupled structure to generate an extra zero between harmonics [5], folded hairpin structure and new coupling scheme to improve performance and reduce size [6], [7], cross-coupled arrangement for sharpen passband skirts [8], and pseudo interdigital coupling structure to reduce size and improve stopband rejection [9]. All above techniques, the resonators were still large due to they were designed with electrical length of λ/2. The slow-wave open-loop resonators [10–12] were also proposed for harmonics suppression and size reduction smaller than half a wavelength. In addition, the SIRs with capacitive load at the end were proposed for dual band [13] and triple band [14] responses, resulting in further size reduction from λ/2 to λ/4. Whereas, the technique using interdigital capacitor seems to have higher capacitance than capacitive load, therefore, novel microstrip interdigital bandstop filters [15], dual-mode BPF based on interdigital [16] were presented, resulting in further size reduction.

In order to improve the filter performances, the cross coupling technique was employed with open-loop resonators [17] and hairpin resonators [18]. The synthesis of cross-coupled resonators was done by [19]. This technique can improve the insertion loss and out-of-band responses due to transmission zero appearance. Also, the technique of overlap cross coupling was proposed for more improvement of insertion loss value at higher frequency to be lower than 3 dB [13].

In this paper, we have developed from step- impedance resonator that can control harmonic frequency as desired for triple-band BPF and taken interdigital capacitor that can reduce size of the resonators. The proposed technique can reduce the resonator size from $\lambda/2$ to $\lambda/8$, which it is the most compact size compared with other transmission line resonators in literatures. In addition, the techniques of multi-section feeding for multiband matching [20], [21] and overlap cross coupling for insertion loss reduction will be applied. The proposed filter can response for multiband operation of GSM, Wi-MAX, and WLAN systems. The details of filter design will be shown in the next section. Then, the proposed filter will be implemented and meas-

ured as detailed in Sec. 3. Finally, conclusion will be in the last section.

2. Filter Design

2.1 Step-impedance Resonator with Interdigital Capacitor

The proposed multiband BPF has been designed on the GML 1000 substrate with relative permittivity ε_r of 3.2, loss tangent of 0.004 and thickness of 0.762 mm. Structure of the proposed filter is shown in Fig. 1, consisting of four resonators connected by using overlap cross coupling technique. Each resonator has been designed using step-impedance resonator (SIR) with interdigital capacitors at both ends as illustrated in Fig. 2(a). The desired fundamental, first, and second harmonic resonances appear at 1.8 GHz, 3.7 GHz, and 5.2 GHz, respectively; the simulated result by IE3D software is shown in Fig. 3.

The interdigital capacitor structure connected with SIR can reduce size of the filter which it can control the

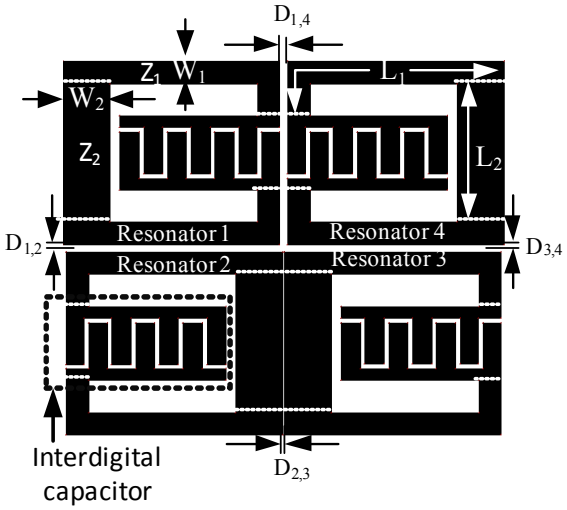

Fig. 1. Multiband BPF structure.

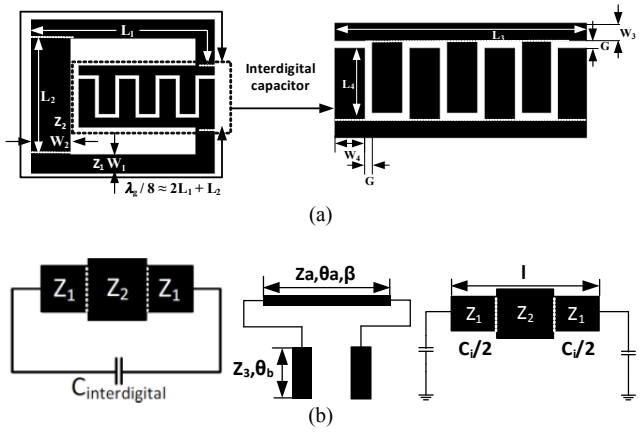

Fig. 2. Step-impedance resonator with interdigital structure: (a) geometrical diagram and (b) equivalent circuit.

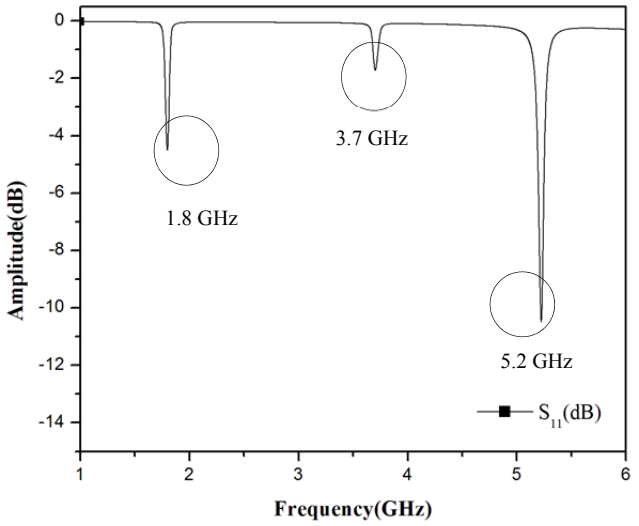

Fig. 3. Simulated result of SIR with interdigital capacitor.

second and third resonances. It is found that this technique can reduce the electrical length of resonators from $\lambda_g/2$ to $\lambda_g/8$. In Fig. 2(a), the characteristic impedances of SIR in the transmission line are Z_1 and Z_2, Z_3 is the characteristic impedance within interdigital capacitor, C_i is the interdigital capacitor, β is the propagation constant, θ_a is the electrical length of transmission line, θ_b is the electrical length within interdigital capacitor, and l is the length of transmission line. The parameter θ_a is $2(\theta_1 + \theta_2)$. Assuming $\theta_1 = \theta_2 = \theta$, the characteristic impedance (Z_a) can be determined from (1), while the impedance relation ratio (K) is characteristic impedance ratio between Z_1 and Z_2.

$$Y_a = \frac{1}{Z_a} = jY_2 \frac{2(1+K)(K-\tan^2\theta)\tan\theta}{K-2(1+K+K^2)\tan^2\theta + K\tan^4\theta}. \quad (1)$$

Figure 2(b) shows the equivalent circuit of this resonator, which can be determined from ABCD matrix [22]. The parameters Z_a and C_i are related to three resonant frequencies that can be determined as

$$C_i = \frac{(\varepsilon_r + 1)}{L_1}) L_4 (\varepsilon_r + 1)[0.1(n-3) + 0.11], \quad (2)$$

$$\theta_{a0} = 2 \tan^{-1}\left(\frac{1}{\pi f_1 Z_a C_i}\right), \quad (3a)$$

$$\theta_{a1} = 2\pi - 2 \tan^{-1}(\pi f_1 Z_a C_i), \quad (3b)$$

$$\theta_{a2} = 2 \tan^{-1}\left(\frac{1}{\pi f_3 Z_a C_i}\right). \quad (3c)$$

Then, the designed resonator parameters can be obtained as follows: $W_1 = 1.15$ mm, $W_2 = 2.39$ mm, $W_3 = 0.578$ mm, $W_4 = 0.975$ mm, $L_1 = 13.885$ mm, $L_2 = 7.03$ mm, $L_3 = 8.192$ mm, and $L_4 = 2.357$ mm. The resonator size is approximately $\lambda/8$. It has been found that the proposed filter has a smaller size compared with the recent published filer designs that has the resonator size of about $\lambda/4$ [14]. However, most of the designed filters have the resonator sizes of $\lambda/2$ at the fundamental frequency [1].

2.2 Cross-coupled Structure

The structure of cross-coupled multiband BPF consists of four step-impedance interdigital capacitor resonators. The cross-coupled technique is used to design the proposed filter which can improve matching, resulting in lower insertion loss. The determined coupling coefficient between a pair of resonators can be found by using

$$K_{ij} = \frac{f_h^{\,2} - f_l^{\,2}}{f_h^{\,2} + f_l^{\,2}} \tag{4}$$

where f_l and f_h are lower and higher peak frequencies of the simulated response, respectively. To calculate both values, the coupled distance between a pair of resonators must be tuned, resulting in the double peak response [22], [23]. From the coupling effect of our proposed filter, these values can be investigated by simulation using full wave method of moment (MOM) software package from IE3D.

The coupling distances $D_{1,2}$, $D_{1,4}$, $D_{2,3}$ and $D_{3,4}$ and coupling coefficients can be simulated for each pair of resonators. Graphs obtained from simulation can be classified into three types as electric coupling, magnetic coupling, and mix coupling as depicted in Figs. 4 (a) to (c). Each graph has information for three frequencies: 1.8 GHz, 3.7 GHz and 5.2 GHz. Curves of each frequency are intersected at the same point of coupling coefficient and coupling distance. Considering these three graphs in Figs. 4 (a) to (c), the coupling coefficients between resonators can be estimated as follows: $k_{12} = k_{34} = 0.02$, $k_{23} = 0.02$ and $k_{14} = 0.013$ and the distance D can be obtained from these graphs as well.

The distance from these graphs are adjusted or optimized by IE3D program to obtain the distance D for appropriate frequency responses. After optimization, the appropriate distances $D_{12} = D_{34} = 0.56$ mm, $D_{23} = 0.76$ mm, and $D_{14} = 0.67$ mm.

The designed filter as shown in Fig. 1 is taken to connect with 50 Ω feed that the simulated result is as shown in Fig. 5. There are insertion losses of –2.645 dB, –2.343 dB, –3.242 dB and return losses of –19.245 dB, –14.237 dB, –24.693 dB at the frequencies of 1.8 GHz, 3.7 GHz, and 5.2 GHz, respectively. The insertion loss at the second harmonic is about –3 dB, then overlap coupling technique has been utilized for improvement.

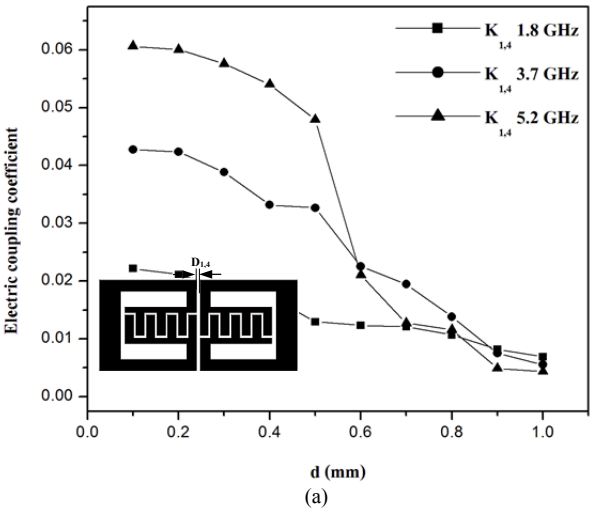

(a)

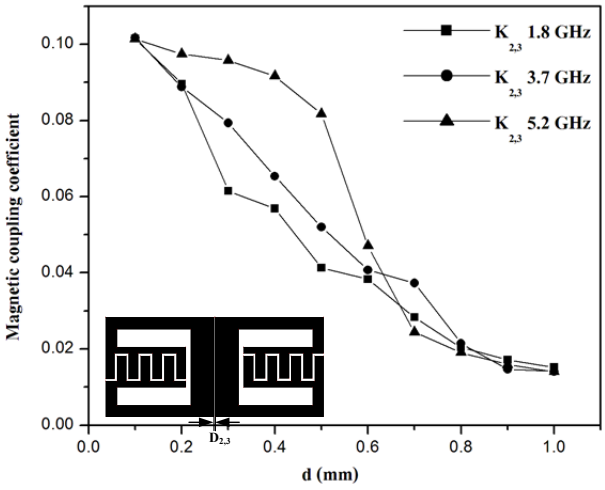

(b)

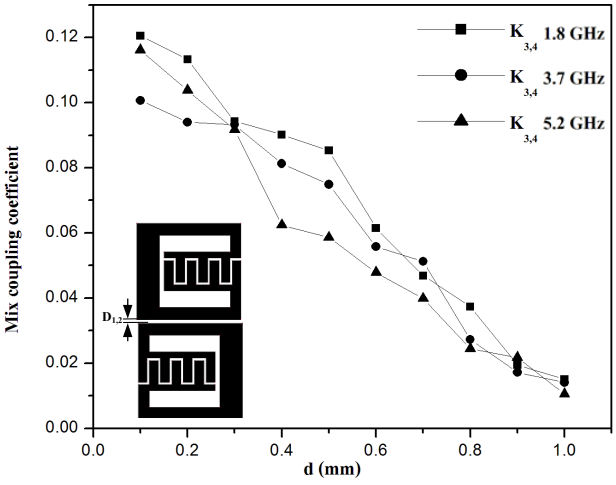

(c)

Fig. 4. Coupling coefficients of the proposed filter: (a) Electric coupling, (b) Magnetic coupling, and (c) Mixed coupling.

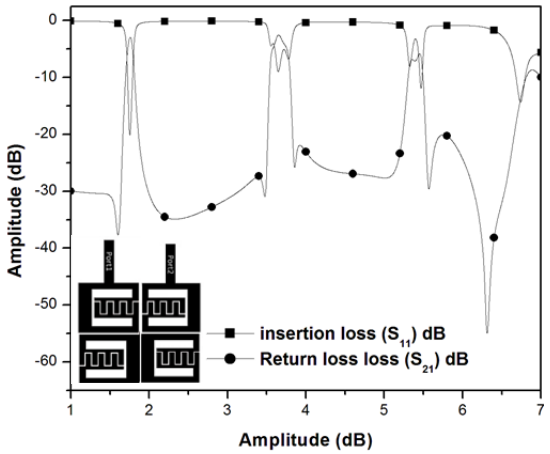

Fig. 5. The structure and result with 50 Ω feeding line.

2.3 Overlap Cross Coupling

After connecting the resonators with 50 Ω feeds as shown in Fig. 5, it has been found that the result has not matched at the second and third harmonic frequencies. The multi-section feeds have been then proposed to connect multiband resonators [21]. The feeds consist of tapered and multi-step sections, whose characteristic impedance corresponds to those operations L and C. The designed multi-section feeding line parameters can be obtained as follows: W_5 = 8.3975 mm, W_6 = 1.8 mm, W_7 = 1.5244 mm, W_8 = 0.6244 mm, W_9 = 0.2 mm, W_{10} = 0.25 mm, W_{11} = 0.15 mm, W_{12}= 0.0.95 mm, W_{13}= 5.95 mm, W_{14}= 0.8 mm, W_{15}= 4.971 mm, L_5= 1.3124 mm, L_6= 3.25 mm, L_7= 3.05 mm, L_8= 0.7 mm, L_9= 1.555 mm, L_{10}= 1.7 mm, L_{11}= 2.345 mm, L_{12}= 1.625 mm, L_{13}= 1.45 mm, L_{14}= 1.222 mm, L_{15}= 1.454 mm, L_{16}= 1.4276 mm, L_{17}= 10.59 mm, and L_{18}= 3.185 mm, as shown in Fig. 6(a). This multi-section feeding line has a low-pass characteristic and can perform as matching network covering all designed frequency bands, resulting in the characteristic improvement for the second and third bands. The simulated result of the proposed filter with multi-section feeds is shown in Fig. 6(b).

The group delay, time domain performance, of the proposed filter can be analyzed. Figure 7 shows the simulated group delay of the proposed filter. It is shown that the

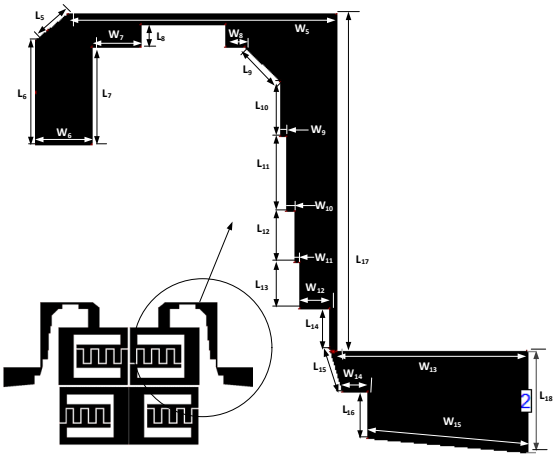

(a)

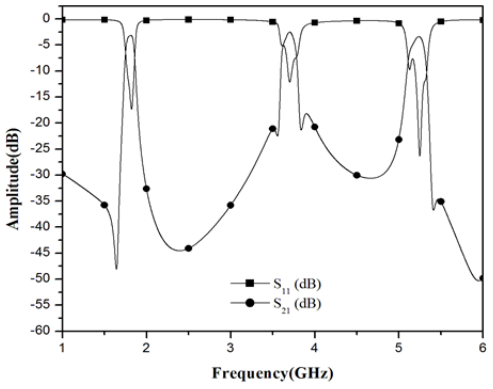

(b)

Fig. 6. The BPF with multi-section line: (a) the details of designed feeding line and (b) the simulated result.

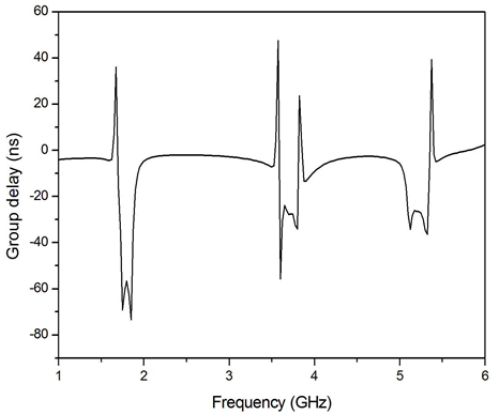

Fig. 7. Group delay of the multiband BPF.

simulated group delays are constant over three desired passbands, which are about –60 ns at the fundamental frequency band and about –25 ns at both harmonic frequency bands. The negative values could be caused by the slow wave effect. However, this can guarantee that fundamental and harmonic frequency bands can be controlled as desired and the proposed filter can work very well for all bands.

Then, the overlap coupling technique [10] can be used by shifting up and down the resonators 3 and 4 along the vertical axis with a distance of h as shown in Fig. 8. The distance h is varied between 0.5 to 2.0 mm with constant coupling coefficients (D_{12}, D_{23}, D_{34}, and D_{14}). The results of each resonant frequency are illustrated in Fig. 9. It can be clearly seen that at odd frequencies (1.8 GHz, and 5.2 GHz), the effects by varying parameter h are displayed in Fig. 9(a) and Fig. 9(c) whereas even frequency is not affected obviously when varying parameter h as shown in Fig. 9(b). In Fig. 9(a), it is found that the return loss (S_{11}) is approximate –10 dB and the insertion loss (S_{21}) is about –3 dB; however, at h = 0.5 mm, the return loss (S_{11}) is less than –20 dB. In Fig. 9(b), the insertion loss (S_{21}) and the return loss (S_{11}) are slightly changed by varying parameter h. Finally, Fig. 9(c) shows the return loss (S_{11}) less than –10 dB and insertion loss (S_{21}) nearby –3 dB; nevertheless, at h = 0.5 mm, the return loss (S_{11}) is less than –20 dB. It can be summarized that overlap parameter h = 0.5 mm is the best choice for insertion loss improvement of the proposed filter as shown in Fig. 9. The insertion loss and return loss caused by overlap coupling are demonstrated in Tab. 1.

3. Implementation and Results

After designing the multiband BPF by techniques as mentioned, this section presents and discusses property of coupling between resonators connected by cross coupling. There are appropriated parameters of coupling between resonators as $D_{12} = D_{34}$ = 0.56 mm, D_{23} = 0.76 mm and D_{14} = 0.67 mm. The illustration of overlap coupling between resonators 3 and 4 along vertical axis has been done by simulation of electric and magnetic fields at all frequency ranges using IE3D program as results shown in Figs. 11–13 where increasing coupling coefficient results to insertion

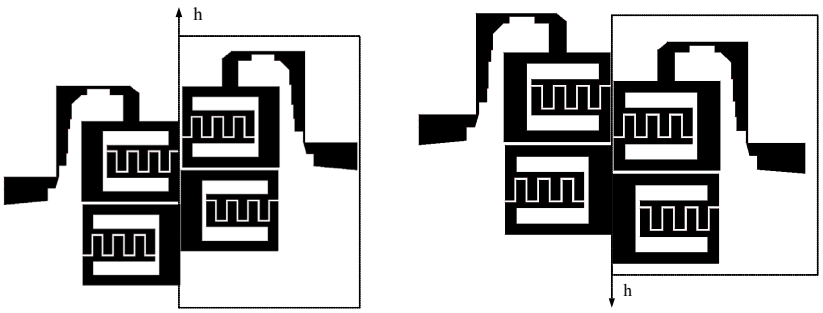

Fig. 8. Shifting of resonators 3 and 4 along vertical axis with distance (a) *h* and (b) *–h*.

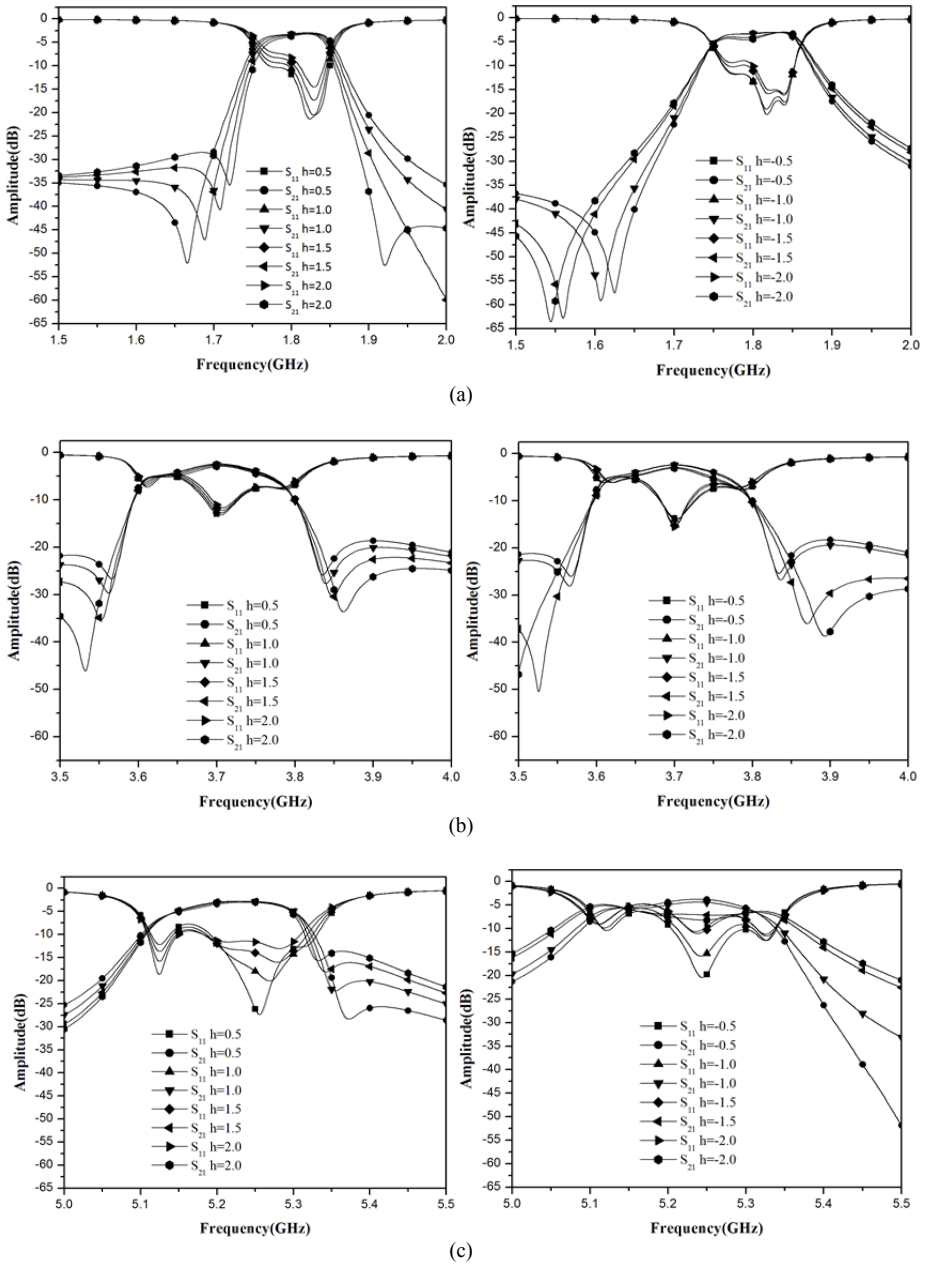

Fig. 9. S-parameters for varying distance *h* and *–h* at (a) 1.8 GHz, (b) 3.7 GHz, and (c) 5.2 GHz.

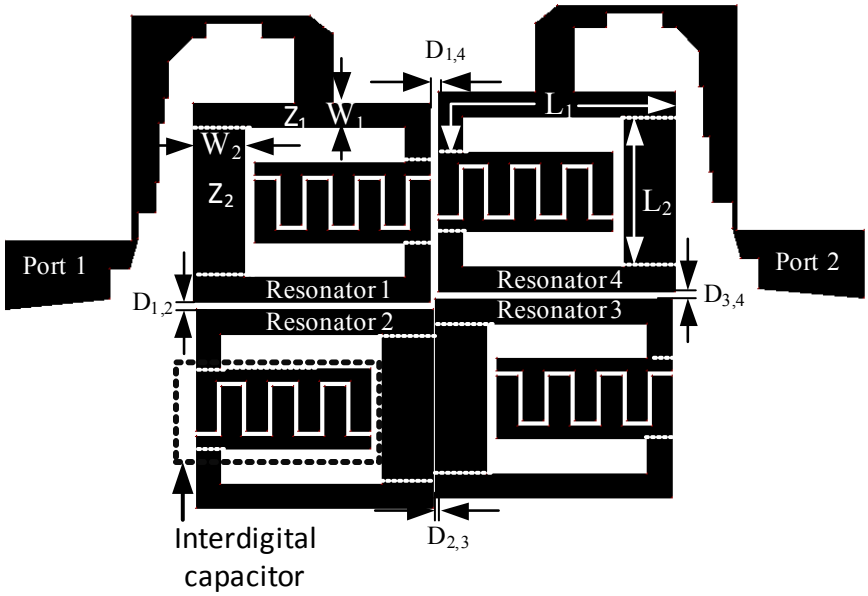

Fig. 10. The proposed overlap cross-coupled band-pass filter.

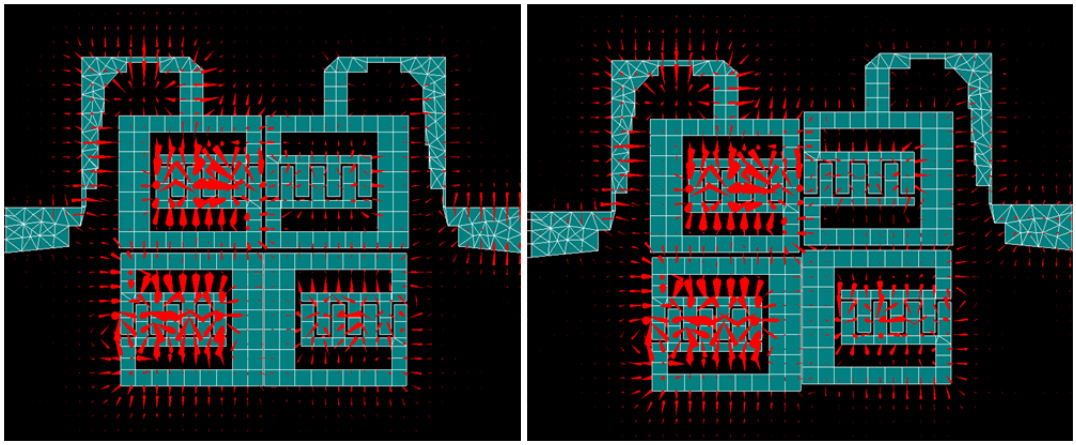

(a)

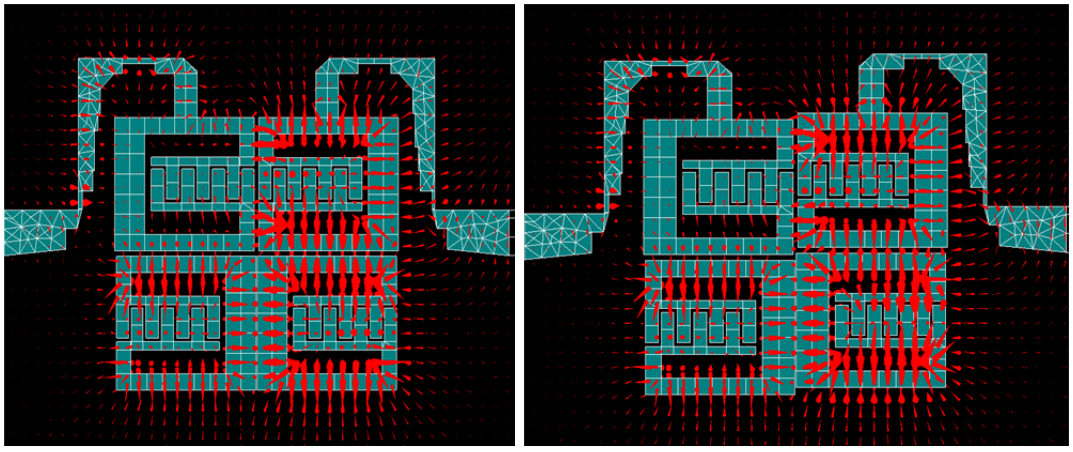

(b)

Fig. 11. Simulation results of proposed filter at 1.8 GHz: (a) electric field and (b) magnetic field.

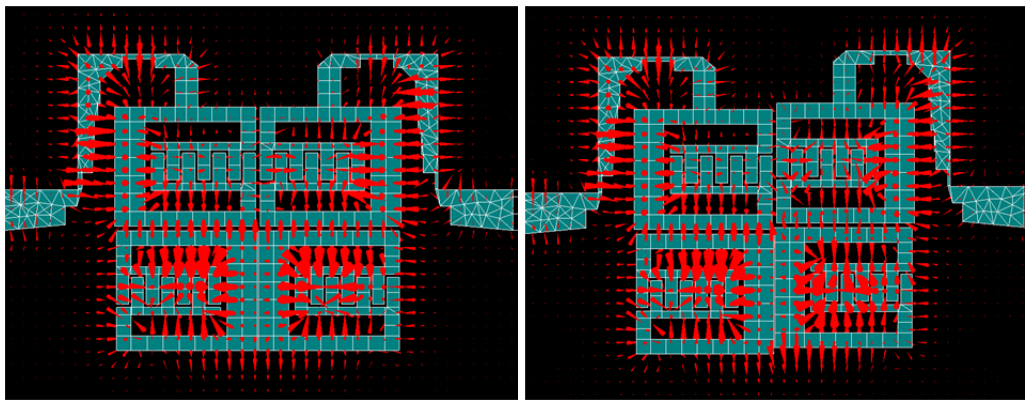

(a)

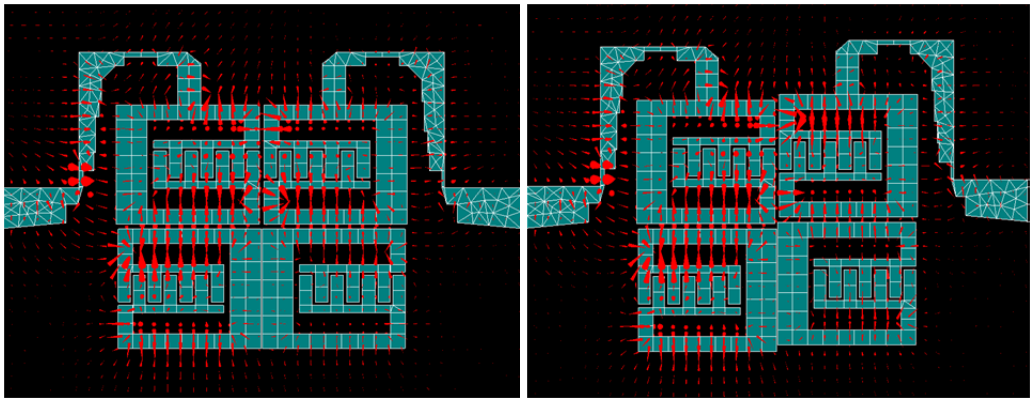

(b)

Fig. 12. Simulation results of the proposed filter at 3.7 GHz: (a) electric field and (b) magnetic field.

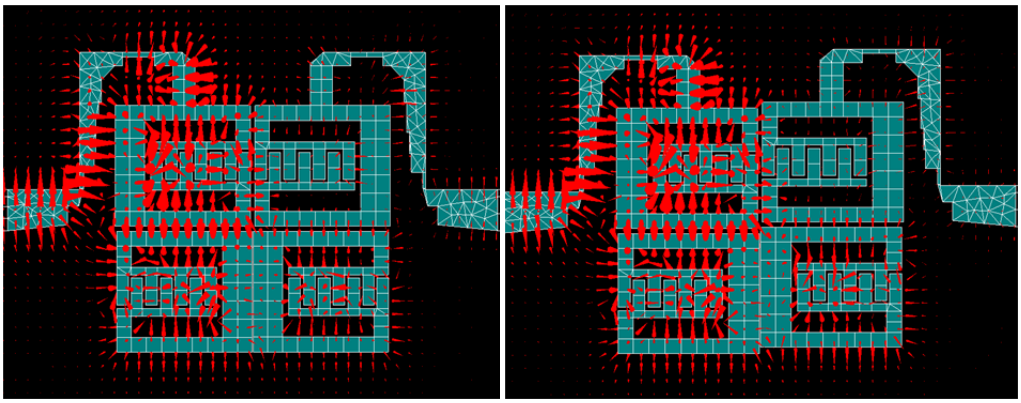

(a)

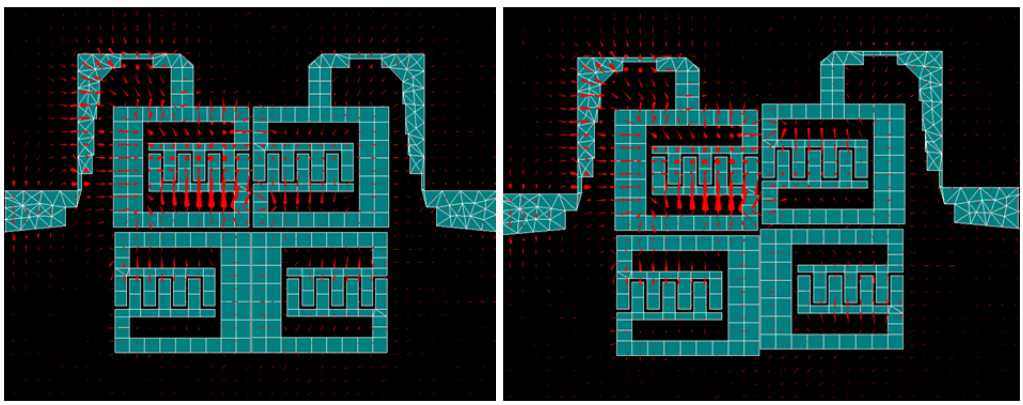

(b)

Fig. 13. Simulation result of proposed filter at 5.2 GHz: (a) electric field and (b) magnetic field.

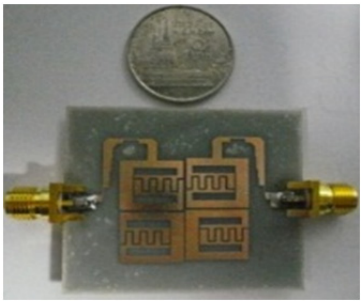

Fig. 14. A photograph of the proposed BPF.

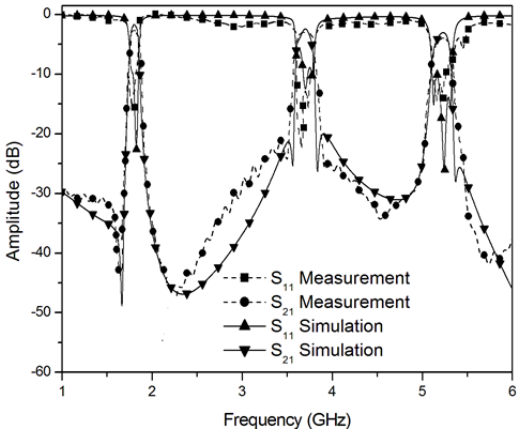

Fig. 15. Comparison results of simulated and measured responses of S_{11} and S_{21}.

Type of Loss \ Range of Frequency		1.8 GHz	3.7 GHz	5.2 GHz
Insertion loss (S_{21}) dB	**None Overlap Coupling**	–2.645	–2.343	–3.242
	Overlap Coupling	–2.642	–2.398	–2.742
Return loss (S_{11}) dB	**None Overlap Coupling**	–19.245	–14.237	–24.693
	Overlap Coupling	–20.864	–13.864	–24.568

Tab. 1. Comparison results of simulated responses of cross coupling and overlap coupling.

loss (S_{21}) lower than 3 dB. There are three types of cross couplings as electric, magnetic and mix couplings. Normally, there are transmission fields from resonator 1 to resonator 2, resonator 2 to resonator 3, and resonator 3 to resonator 4. There is no transmission field between resonator 1 to resonator 3 and resonator 2 to resonator 4.

At fundamental frequency (1.8 GHz) as seen in Fig. 11, it is found that the gap between resonators 1 and 4 on the left side of Fig. 11(a) has electric coupling. Also, there is E-field between resonators 1 and 4 more than E-field between resonators 2 and 3, which the structure has magnetic coupling. While the H-field between resonators 2 and 3 is higher than the H-field between resonators 1 and 4 as shown on the right side of Fig. 11(a). After shifting up the resonators 3 and 4 along vertical axis as shown in Fig. 11(b), the E-field and H-field are similar to Fig. 11(a). There are cross fields between resonators 1 and 3, and between resonators 2 and 4, which are called mix coupling. Because there are E-field and H-field concomitant, when increasing overlap coupling distance, mix coupling has been increased. This will result in improvement of insertion loss value. However, at fundamental frequency 1.8 GHz, there is less cross coupling, the insertion loss improvement could not be noticed as shown in Fig. 8(a). At the second harmonic frequency (3.7 GHz), the E-field and H-field are displayed in Figs. 12(a) and (b), respectively. The cross coupling fields between resonators 1 and 3, and between resonators 2 and 4 when overlap at the second harmonic frequency is higher than the fundamental frequency. As a result, the insertion loss at the second harmonic frequency is improved comparing with the fundamental frequency as shown in Fig. 9(b). At the third harmonic frequency (5.2 GHz), both E-field and H-field are shown in Figs. 13(a) and (b), respectively. It has been found that there is strong effect of cross coupling when overlap compared with the fundamental and second harmonic frequencies, resulting in more improvement in insertion loss as shown in Fig. 9(c). It can be concluded that the cross coupling fields caused by overlap resonators have more effect at higher frequency and less effect at low frequency.

After all, we have fabricated the proposed multi-band BPF with the size of 4×2.3 cm^2 as shown in Fig. 14. The simulation results show the resonant frequencies at 1.8 GHz, 3.7 GHz, and 5.2 GHz as designed. The values of return losses (S_{11}) at the resonances are –20.86 dB, –13.86 dB, and –24.57 dB, respectively. The values of insertion losses (S_{21}) are –2.64 dB, –2.40 dB, and –2.74 dB, and bandwidth are 110 MHz, 200 MHz, and 220 MHz, respectively. The proposed multi-band BPF was measured by Agilent 8791ES network analyzer, resulting in the same resonant frequencies as simulated. From the measurement results, the values of measured return losses (S_{11}) are –17.6 dB, –19.7 dB, and –15.9 dB, and bandwidth are 121 MHz, 224 MHz, and 233 MHz, respectively. The values of insertion losses (S_{21}) at the resonances are –2.83 dB, –2.82 dB, and –2.96 dB, respectively. The comparison results of simulated and measured responses of return loss and insertion loss are shown in Fig. 15. It is clearly seen that the simulated and measured resonant results are at the same frequencies. Moreover, values of both measurement insertion losses and return losses are almost similar to simulation.

4. Conclusions

A compact multi-band BPF using overlap coupling of step-impedance with interdigital capacitor resonators has been proposed to operate at 1.8 GHz, 3.7 GHz, and 5.2 GHz, respectively. This proposed BPF has the most compact size comparing with the recent BPF whose size can be reduced from $\lambda/2$ to $\lambda/8$. The results show good agreement between simulation and measurement with return loss more than 10 dB and insertion loss less than 3.0 dB. The filter also demonstrates good performances and it can support GSM, Wi-MAX, and WLAN systems. However, the filter bands can be adjusted to any frequency corresponding to application bands by changing the resonator lengths and interdigital capacitive values.

Acknowledgments

This work has been supported by the Thailand Research Fund through the TRF Senior Research Scholar Program Grant No. RTA5780010 and the Department of Electrical and Computer Engineering, Faculty of Engineering, King Mongkut's University of Technology North Bangkok under the grant contract number FoE 167/2014 (ECE-RA). The authors would also like to acknowledge Pathumwan Institute of Technology in Thailand for the usage of simulation software.

References

[1] APRIYANA, A. A. A., PING, Z. Y. A dual-band BPF for concurrent dual-band wireless transceiver. In *Proceedings of the 5th Electronics Packaging Technology Conference*, 2003, p. 143–145. DOI: 10.1109/EPTC.2003.1271506

[2] CHANG, S.-F., JENG, Y.-H., CHEN, J.-L. Dual-band step-impedance bandpass filter for multimode wireless LAN. *IEEE Electronics Letters*, 2004, vol. 40, no. 1, p. 38–39. DOI: 10.1049/el:20040065

[3] KUO, J. T., YEH, T.-H., YEH, C.-C. Design of microstrip bandpass filter with a dual-passband response. *IEEE Transactions on Microwave Theory and Techniques*, 2005, vol. 53, no. 4, p. 1331–1337. DOI: 10.1109/TMTT.2005.845765

[4] LIN, X. M., CHU, Q. X. Design of triple-band bandpass filter using tri-section stepped-impedance resonators. In *International Conference on Microwave and Millimeter Wave Technology (ICMMT 2007)*. Guilin (China), 2007, p. 1–3. DOI: 10.1109/ICMMT.2007.381479

[5] CHEN, Y.-C., HSIEH, Y.-H., LEE, C.H., HSU, C.-I. G. Tri-band microstrip BPF design using tri-section SIRs. In *Antennas and Propagation Society International Symposium*. Honolulu (HI, USA), 2007, p. 3113–3116. DOI: 10.1109/APS.2007.4396195

[6] YANG, X., DAI, L., ZHOU, R. The tri-band filter design based on SIR. In *International Conference on Audio, Language and Image Processing (ICALIP 2008)*. Shanghai, 2008, p. 211–214. DOI: 10.1109/ICALIP.2008.4589998

[7] CHU, Q.-X., LIN, X. M. Advanced triple-band bandpass filter using tri-section SIR. *IEEE Electronics Letters*, Feb 2008, vol. 44, no. 4, p. 295–296. DOI: 10.1049/el:20083096

[8] HSU, C.-I. G., LEE, C.-H., HSIEH, Y.-H. Tri-band bandpass filter with sharp passband skirts designed using tri-section SIRs. *IEEE Microwave and Wireless Components Letters*, 2008, vol. 18, no. 1, p. 19–21. DOI: 10.1109/LMWC.2007.911976

[9] CHEN, F. C., CHU, Q. X. Design of compact tri-band bandpass filters using assembled resonators. *IEEE Transactions on Microwave Theory and Techniques*, 2009, vol. 57, no. 1, p. 165–171. DOI: 10.1109/TMTT.2008.2008963

[10] HONG, J. S., LANCASTER, M. J. Theory and experiment of novel microstrip slow-wave open-loop resonator filters. *IEEE Transactions on Microwave Theory and Techniques*, 1997, vol. 45, no. 12, p. 2358–2365. DOI: 10.1109/22.643844

[11] HONG, J. S., LANCASTER, M. J. End-coupled microstrip slow-wave resonator filter. *IEEE Electronics Letters,* 1996, vol. 32, no. 16, p. 1494–1496. DOI: 10.1049/el:19960959

[12] GU, J., ZHANG, F., WANG, C., et al. Miniaturization and harmonic suppression open-loop resonator bandpass filter with capacitive terminations. In 2006 IEEE MTT-S International Microwave Symposium Digest. San Francisco (CA, USA), June 2006, p. 373–376. DOI: 10.1109/MWSYM.2006.249547

[13] CHOMTONG, P., MAHATTHANAJATUPHAT, C., AKKARAEKTHALIN, P. A dual-band bandpass filter with overlap step-impedance and capacitively loaded hairpin resonators for wireless LAN system. *Hindawi International Journal of Microwave Science and Technology*, 2011, 9 p. DOI: 10.1155/2011/812078

[14] CHOMTONG, P., AKKARAEKTHALIN, P. A triple band bandpass filter using tri-section step-impedance and capacitively loaded step-impedance resonators for GSM, WiMAX, and WLAN systems. *Frequenz Journal,* 2014, vol. 68, no. 5–6, p. 227–234. DOI: 10.1515/freq-2013-0126

[15] YANG, R.-Y., WENG, M.-H., HUNG, C.-Y., et al. Novel compact microstrip interdigital bandstop filters. *IEEE Transactions on Ultrasonics, Ferroelectrics and Frequency Control*, 2004, vol. 51, no. 8, p. 1022–1025. DOI: 10.1109/TUFFC.2004.1324407

[16] XU, F.-L., LIU, X.-G., GUO, H.-P., et al. A compact dual mode BPF based on interdigital structure. In *Proceeding of the IEEE Microwave and Millimeter Wave Technology International Conference (ICMMT)*. Chengdu (China), 2010, p. 1595–1597. DOI: 10.1109/ICMMT.2010.5524850

[17] HONG, J. S., LANCASTER, M. J. Couplings of microstrip square open loop resonators for cross-coupled planar microwave filters.

IEEE Transactions on Microwave Theory and Techniques, 1996, vol. 44, no. 11, p. 2099–2109. DOI: 10.1109/22.543968

[18] HONG, J. S., LANCASTER, M. J. Cross–coupled microstrip hairpin resonator filter. *IEEE Transactions on Microwave Theory and Techniques*, 1998, vol. 46, no. 1, p. 118–122. DOI: 10.1109/22.654931

[19] AMARI, S. Synthesis of cross-coupled resonator filters using an analytical gradient-based optimization technique. *IEEE Transactions on Microwave Theory and Techniques*, 2000, vol. 48, no. 9, p. 1559–1564. DOI: 10.1109/22.869008

[20] COLLIN, R. E. Theory and design of wide-band multisection quarter-wave transformers. *Proceedings of the IRE*, Feb. 1955, vol. 43, no. 2, p. 179–185. DOI: 10.1109/JRPROC.1955.278076

[21] MEESOMKLIN, S. CHOMTONG, P., AKKARAEKTHALIN, P. A multi-section and tapered feeding system for multiband BPF. In *Proceedings of the Asia-Pacific Conference on Antenna and Propagation (APCAP 2013)*. Chiangmai (Thailand), August 2013.

[22] HONG, J. S. *Microstrip Filters for RF/Microwave Applications*. Hoboken (NJ, USA): John Wiley & Sons, 2011. ISBN: 978-0-470-40877-3

[23] SWANSON, D. G. Jr. Narrow-band microwave filter design. *IEEE Microwave Magazine*, 2007, vol. 8, no. 5, p. 105–114. DOI: 10.1109/MMM.2007.904724

About the Authors ...

Suwaluck MEESOMKLIN was born in Bangkok, Thailand. She received B.Eng. and M.Eng degrees in Electrical Engineering from King Mongkut's University of Technology North Bangkok (KMUTNB), Thailand, in 2011 and 2013, respectively. In 2014, she has studied for Ph.D. degree in Electrical Engineering at the same university. Her research interests include passive and active microwave circuits, wideband and multiband antennas, and telecommunication systems.

Pongsathorn CHOMTONG was born in Nonthaburi, Thailand. He received M.Eng. and Ph.D. degrees in Electrical Engineering from King Mongkut's University of Technology North Bangkok (KMUTNB), Thailand, in 2006 and 2011, respectively. In 2012, he joined the Dept. of Teacher Training in Electrical Engineering, KMUTNB, as an instructor. His current research interests include passive and active microwave circuits, wideband and multiband antennas, and telecommunication systems. He is a member of IEEE.

Prayoot AKKARAEKTHALIN received the B.Eng. and M.Eng. degrees in Electrical Engineering from King Mongkut's University of Technology North Bangkok (KMUTNB), Thailand, in 1986 and 1990, respectively, and the Ph.D. degree from the University of Delaware, Newark, USA, in 1998. From 1986 to 1988, he worked in the Microtek Laboratory, Thailand. In 1988, he joined the Department of Electrical Engineering, KMUTNB. His current research interests include passive and active microwave circuits, wideband and multiband antennas, and telecommunication systems. Dr. Prayoot is a member of IEEE, IEICE Japan, ECTI, EEAAT Thailand. He was the Chairman for the IEEE MTT/AP/ED Thailand Joint Chapter during 2007 and 2008. He is now the president for ECTI Association, Thailand.